Available online at www.sciencedirect.com
SCIENCE DIRECT®
Acta Materialia 52 (2004) 1155–1162
Acta MATERIALIA
www.actamat-journals.com

Modeling the austenite–ferrite diffusive transformation during continuous cooling on a mesoscale using Monte Carlo method

Mingming Tong *, Dianzhong Li, Yiyi Li

Institute of Metal Research, No. 8 Res. Lab., Chinese Academy of Sciences, 72 Wenhua Road, Shenyang 110016, PR China

Received 14 August 2003; received in revised form 4 November 2003; accepted 5 November 2003

Abstract

A Q-state Potts model is adopted to simulate the austenite–ferrite diffusive transformation during continuous cooling in a low carbon steel on a mesoscale with Monte Carlo method. The effects of the interfacial energy and the carbon diffusion on the phase transformation are both taken into account. The consideration of the interfacial energy effect makes the simulated ferrite grains polygonal. To simulate the carbon diffusion during the process of phase transformation, a random jumping based mesocopic diffusion model is developed. In this paper, the evolutions of the microstructure and the carbon concentration field are simulated. The simulation results of the effects of the cooling rate on the volume fraction of the ferrite and the ferrite grain size agree well with the experimental results. The simulation results show that increasing the cooling rate is an effective way to refine the microstructure. This Monte Carlo simulation technique provides a novel way for investigating the diffusive transformation on a mesoscale.

Keywords: Monte Carlo; Diffusive transformation; Mesoscale; Continuous cooling

1. Introduction

Because the austenite–ferrite diffusive transformation is of great importance nowadays especially in the steel industry, it has already been investigated intensively during recent years. Many researchers have developed number of methods to simulate it [1–3]. One of the most important models for modeling the austenite–ferrite diffusive transformation is to numerically solve the diffusion equation in a representative domain of the microstructure [4–7]. By numerically solving the diffusion equation, Jacot and Rappaz [8,9] have adopted a finite volume method to simulate the diffusion of solute atoms and corresponding phase transformation in a two-dimensional domain. Their model has been successfully applied to the austenization of hypoeutectoid steels during the reheating. Based on the finite volume method, a cellular automaton (CA) model [10–13] is developed to simulate the austenite-to-ferrite transformation during continuous cooling in a low-carbon steel. Though those finite volume method based simulation works have already been successfully applied to the austenite–ferrite diffusive transformation, some assumptions in those models still seem questionable. First of all, the effect of the interfacial energy (phase boundary energy or grain boundary energy) on the phase transformation is neglected. In fact, the interfacial energy takes great effect on the austenite–ferrite diffusive transformation. The nucleation and the growth of a new phase will enlarge the area of the phase boundaries. The increase of the phase boundary energy will restrain this nucleation and growth. The solute diffusion between the matrix and the new phase, however, promotes the transformation. The phase transformation is dominated by the competition between the interfacial energy and the chemical free energy. Therefore, neglecting the effect of the interfacial energy on the phase transformation seems questionable. Second, the carbon concentrations of ferrite grains are assumed to be the same homogeneous values as determined by the Fe–C binary equilibrium phase diagram. This assumption is only valid when the system is cooled at a cooling rate low enough.

* Corresponding author. Tel.: +86-24-23971973; fax: +86-24-2389 1320.
E-mail address: mmtong@imr.ac.cn (Mingming Tong).

1359-6454/$30.00 © 2003 Acta Materialia Inc. Published by Elsevier Ltd. All rights reserved.
doi:10.1016/j.actamat.2003.11.006

The system that experiences a continuous cooling at a high cooling rate will significantly deviate its equilibrium state. The carbon concentration of the ferrite deviates the theoretic value predicted by the Fe–C binary equilibrium phase diagram in reality. The Monte Carlo (MC) method is a statistic model. It has been widely used to model the microstructure evolution in materials such as the grain growth [14] and the recrystallization [15] on a mesoscale. In the MC method, the evolutions of the microstructure and the carbon concentration field proceed in the manner of Metropolis sampling. In this paper, a Q-state Potts model is adopted to simulate the austenite ferrite diffusive transformation in a low carbon steel during continuous cooling on a mesoscale using MC method. In the Q-state Potts model, the effects of the interfacial energy and the carbon diffusion on the evolution of the system are both taken into account by dint of the interfacial energy term and the chemical free energy term of the Hamiltonian of the system. The carbon diffusion is simulated independently on the numerical solution of the diffusion equation.

2. Monte Carlo model and algorithm

The microstructure is mapped onto a two-dimensional hexagonal lattice. Being different from the model of Jacot and Rappaz, a hexagonal cell can only take two different states: ferrite or austenite (see Fig. 1). This means that the width of the grain boundaries and phase boundaries is zero in the MC model in this paper. To describe the state of a MC cell i, there are three parameters. They are the orientation S_i, the carbon concentration C_i and the order parameter η_i, respectively. The orientation is the same as that is defined in the traditional MC simulation of grain growth [14]. The carbon concentration is in the weight percent unit. The order parameter is defined as 0 representing the austenite phase and 0.293 representing the ferrite phase. The evolutions of these three parameters correspond to the evolutions of the microstructure and carbon concentration field. This means that there are three procedures coupled in the simulation of the transformation, which are the orientation transition, the carbon diffusion and the transition of the order parameter.

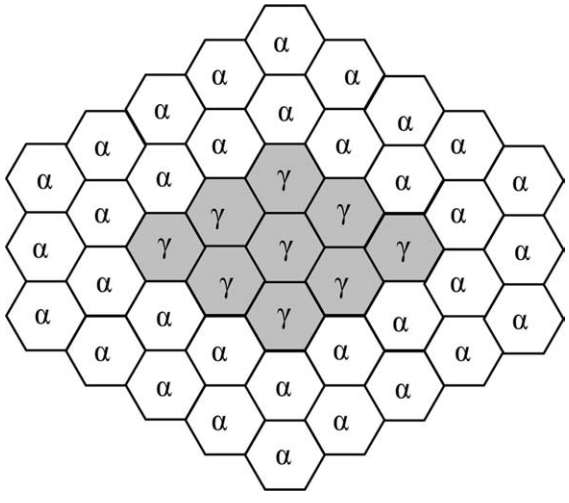

Fig. 1. Schematic illustration of the hexagonal grid used to represent the two phase system.

The austenite–ferrite diffusive phase transformation is dominated by the interaction between the interface migration and the diffusion of solutes. In this paper, the chemical free energy item and the boundary energy term are introduced into Hamiltonian of the system in the Q-state Potts model as follows:

$$H = \frac{1}{2}\sum_{i}^{n}\sum_{j}^{m} G^{\mathrm{b}}_{S_iS_j} + \sum_{i}^{n} G^{\mathrm{c}}_{i}, \tag{1}$$

where G^{c}_i is the chemical free energy of cell i with its orientation S_i; $G^{\mathrm{b}}_{S_iS_j}$ is the boundary energy between MC cell i and cell j with their corresponding orientations.

In each Monte Carlo step (MCS), cell i has to be selected at random and then two cells of its nearest neighbors are determined by random selection as cell j and cell k. j is allowed to be equal to k. Then, the orientation and the order parameter of cell i are changed to the same as those of cell j. After that, the carbon diffusion between cell i and cell k is performed in the way stated in Section 2.1. The Hamiltonians of the system before and after the above transition attempts are stored as H_2 and H_2, respectively. If $H_2 \leqslant H_1$, the transition is definitely accepted. Otherwise, the variation occurs with a probability of $W = \exp\{(H_1 - H_2)/k_{\mathrm{B}}T\}$, where k_{B} is the Boltzman constant and T is the absolute temperature [16].

2.1. Random jump based mesoscopic MC diffusion model

A random number that ranges between zero and the sum of the carbon concentration of cell i and that of cell k is added to the carbon concentration of cell i. Then, the same value is subtracted from the carbon concentration of cell k. This redistribution of the carbon concentration between cell i and cell k by means of the random jump must obey the solute conservation rule. The acceptance of this redistribution is determined by the transition rule stated above. In essence, the mesoscopic diffusion of solute is the mesoscopic effect of the random jump of the solute atoms on a mesoscale. The direction that carbon diffuses towards on the mesoscale is the direction towards which the probability of the occurrence of the random jump of the solute atoms is larger than other directions. This random jump based mesoscopic MC diffusion model is independent on the

equilibrium phase diagram and the numerical solution of the diffusion equation.

2.2. Pearlite formation

As the temperature gradually decreases in the course of the continuous cooling, more and more ferrite grains form. The carbon solutes will build up in the austenite cells neighboring these growing ferrite grains. When the carbon concentration in an austenite cell becomes undercooled with respect to pearlite formation, this austenite cell will transform to a pearlite cell.

2.3. Chemical free energy model

In this paper, the regular solution free energy model is adopted [17–23]. The low carbon steel can be reduced to a Fe–Mn–C ternary system. The mol chemical free energy of the system can be expressed as

$$G_m = x_{\mathrm{Fe}}\mu_{\mathrm{Fe}} + x_{\mathrm{C}}\mu_{\mathrm{C}} + x_{\mathrm{Mn}}\mu_{\mathrm{Mn}}, \tag{2}$$

where x_{Fe}, x_{C} and x_{Mn} are the mol fractions of iron, carbon and manganese, respectively; μ_{Fe}, μ_{C} and μ_{Mn} are the chemical potentials of iron, carbon and manganese in the solution, respectively.

$$\mu_{\mathrm{Fe}} = {}^0G_{\mathrm{Fe}} + RT\ln y_{\mathrm{Fe}} + \frac{c}{a}RT\ln(1-y_{\mathrm{C}}) + {}^{\mathrm{E}}G_{\mathrm{Fe}},$$

$$\mu_{\mathrm{Mn}} = {}^0G_{\mathrm{Mn}} + RT\ln y_{\mathrm{Mn}} + \frac{c}{a}RT\ln(1-y_{\mathrm{C}}) + {}^{\mathrm{E}}G_{\mathrm{Mn}},$$

$$\mu_{\mathrm{C}} = {}^0G_{\mathrm{C}} + RT\ln\frac{y_{\mathrm{C}}}{1-y_{\mathrm{C}}} + {}^{\mathrm{E}}G_{\mathrm{C}},$$

where ${}^0G_{\mathrm{Fe}}$, ${}^0G_{\mathrm{C}}$ and ${}^0G_{\mathrm{Mn}}$ are the mol Gibbs free energy of iron element, carbon element (graphite) and manganese element, respectively. ${}^{\mathrm{E}}G_i$ is the excessive free energy, which can be expressed as

$$\begin{aligned}{}^{\mathrm{E}}G_{\mathrm{Fe}} = {} & -y_{\mathrm{Mn}}y_{\mathrm{C}}\cdot(\Delta G + L^{\mathrm{C}}_{\mathrm{FeMn}} - L^{\mathrm{v}}_{\mathrm{FeMn}} + L^{\mathrm{Mn}}_{\mathrm{Cv}} - L^{\mathrm{Fe}}_{\mathrm{Cv}}) \\ & + y^2_{\mathrm{Mn}}L^{\mathrm{v}}_{\mathrm{FeMn}} + y^2_{\mathrm{C}}L^{\mathrm{Fe}}_{\mathrm{Cv}} + 2y^2_{\mathrm{Mn}}y_{\mathrm{C}}\cdot(L^{\mathrm{C}}_{\mathrm{FeMn}} - L^{\mathrm{v}}_{\mathrm{FeMn}}) \\ & + 2y_{\mathrm{Mn}}y^2_{\mathrm{C}}(L^{\mathrm{Mn}}_{\mathrm{Cv}} - L^{\mathrm{Fe}}_{\mathrm{Cv}}),\end{aligned}$$

$$\begin{aligned}{}^{\mathrm{E}}G_{\mathrm{Mn}} = {} & -y_{\mathrm{Fe}}y_{\mathrm{C}}\cdot(\Delta G + L^{\mathrm{v}}_{\mathrm{FeMn}} - L^{\mathrm{C}}_{\mathrm{FeMn}} + L^{\mathrm{Mn}}_{\mathrm{Cv}} - L^{\mathrm{Fe}}_{\mathrm{Cv}}) \\ & + y^2_{\mathrm{Fe}}L^{\mathrm{v}}_{\mathrm{FeMn}} + y^2_{\mathrm{C}}L^{\mathrm{Mn}}_{\mathrm{Cv}} + 2y^2_{\mathrm{Fe}}y_{\mathrm{C}}\cdot(L^{\mathrm{C}}_{\mathrm{FeMn}} - L^{\mathrm{v}}_{\mathrm{FeMn}}) \\ & + 2y_{\mathrm{Fe}}y^2_{\mathrm{C}}(L^{\mathrm{Fe}}_{\mathrm{Cv}} - L^{\mathrm{Mn}}_{\mathrm{Cv}}),\end{aligned}$$

$$\begin{aligned}{}^{\mathrm{E}}G_{\mathrm{C}} = {} & y_{\mathrm{Mn}}\cdot(\Delta G + L^{\mathrm{C}}_{\mathrm{FeMn}} - L^{\mathrm{v}}_{\mathrm{FeMn}} + L^{\mathrm{Mn}}_{\mathrm{Cv}} - L^{\mathrm{Fe}}_{\mathrm{Cv}}) - 2y_{\mathrm{C}}L^{\mathrm{Fe}}_{\mathrm{Cv}} \\ & + 2y_{\mathrm{Mn}}y_{\mathrm{C}}(L^{\mathrm{Fe}}_{\mathrm{Cv}} - L^{\mathrm{Mn}}_{\mathrm{Cv}}) + y^2_{\mathrm{Mn}}(L^{\mathrm{v}}_{\mathrm{FeMn}} - L^{\mathrm{C}}_{\mathrm{FeMn}}),\end{aligned}$$

$$\Delta G^{\gamma} = -48,500\ \mathrm{J/mol}, \quad \Delta G^{\alpha} = 145,500\ \mathrm{J/mol},$$

$$y_{\mathrm{Fe}} = \frac{x_{\mathrm{Fe}}}{1-x_{\mathrm{C}}}, \quad y_{\mathrm{C}} = \frac{ax_{\mathrm{C}}}{c(1-x_{\mathrm{C}})}, \quad y_{\mathrm{Mn}} = \frac{x_{\mathrm{Mn}}}{1-x_{\mathrm{C}}},$$

a is the amount of the lattice sites in the solution, c is the amount of the interstitial sites in the solution, $a=1, c=1$ in fcc structure, $a=1, c=3$ in bcc structure; L is the interaction parameter between element i and element j, it can be fitted from the corresponding phase diagram as follows:

$$L^{\gamma\mathrm{Fe}}_{\mathrm{Cv}} = -21,058 - 11.581\cdot T(\mathrm{J/mol}), \quad L^{\alpha\mathrm{Fe}}_{\mathrm{Cv}} = 0,$$

$$L^{\gamma\mathrm{Mn}}_{\mathrm{Cv}} = -21,058 - 11.581\cdot T(\mathrm{J/mol}),$$
$$L^{\gamma\mathrm{v}}_{\mathrm{FeMn}} = 730 - 10\cdot T(\mathrm{J/mol}),$$

$$L^{\alpha\mathrm{v}}_{\mathrm{FeMn}} = 19,450 - 12.81\cdot T - 1500({}^0S_{\mathrm{Fe}})_{\mathrm{mag}}(\mathrm{J/mol}),$$
$$L^{\gamma\mathrm{C}}_{\mathrm{FeMn}} = 9230 - 10\cdot T(\mathrm{J/mol}),$$

$$L^{\alpha\mathrm{C}}_{\mathrm{FeMn}} = L^{\alpha\mathrm{v}}_{\mathrm{FeMn}}, \quad L^{\alpha\mathrm{Mn}}_{\mathrm{Cv}} = 0.$$

$({}^0S_{\mathrm{Fe}})$ is the standard magnetism entropy of pure iron, it can be obtained by the regression of the experimental results of Weiss and Tauer [24]:

$$({}^0S_{\mathrm{Fe}})_{\mathrm{mag}} = \frac{1}{(-0.4071 + \frac{1.67\times10^7}{T^{2.5}} + 8.14\times10^{-17}\cdot T^5)}(\mathrm{J/mol}),$$
$$(400\ \mathrm{K} \leqslant T \leqslant 1200\ \mathrm{K}).$$

According to [25–28], the mol Gibbs free energy of carbon element, iron element and manganese element ${}^0G^{\mathrm{graphite}}_{\mathrm{C}} - {}^0H^{298}_{\mathrm{C}}$, ${}^0G_{\mathrm{Fe}} - {}^0H^{298}_{\mathrm{Fe}}$, ${}^0G_{\mathrm{Mn}} - {}^0H^{298}_{\mathrm{Mn}}$, can be obtained. Because we are only interested in the change of free energy caused by the state transition when considering the acceptance of the transition attempt, ${}^0H^{298}_{\mathrm{C}}$, ${}^0H^{298}_{\mathrm{Fe}}$, ${}^0H^{298}_{\mathrm{Mn}}$ can be assumed to be equal to zero for the convenience of the calculation.

The chemical free energy of cell i can be written as, $G^{\mathrm{c}}_i = G_m\cdot M_i$, where M_i is the mol of the substance of cell i.

2.4. Boundary energy

If the boundary is a grain boundary, the boundary energy between cell i and j can be written as [29,30]

$$G^{\mathrm{b}}_{S_iS_j}(\theta) = \begin{cases} J\dfrac{\theta^\circ}{\theta^*}\left[1-\ln\left(\dfrac{\theta^\circ}{\theta^*}\right)\right] * a, & \theta^\circ < \theta^*, \\ J * a, & \theta^\circ \geqslant \theta^*, \end{cases} \tag{3}$$
$$\begin{cases} \theta^\circ = |\theta_{ij}|, & 0 \leqslant |\theta_{ij}| \leqslant \pi, \\ \theta^\circ = 2\pi - |\theta_{ij}|, & \pi \leqslant |\theta_{ij}| \leqslant 2\pi. \end{cases}$$

If the boundary is a phase boundary, the boundary energy between cell i and j can be written as

$$G^{\mathrm{b}}_{S_iS_j}(\theta) = \begin{cases} \frac{1}{2}J + \frac{1}{2}J\dfrac{\theta^\circ}{\theta^*}\left[1-\ln\left(\dfrac{\theta^\circ}{\theta^*}\right)\right] * a, & \theta^\circ < \theta^*, \\ J * a, & \theta^\circ \geqslant \theta^*, \end{cases}$$
$$\begin{cases} \theta = |\theta_{ij}|, & 0 \leqslant |\theta_{ij}| \leqslant \pi, \\ \theta = 2\pi - |\theta_{ij}|, & \pi \leqslant |\theta_{ij}| \leqslant 2\pi, \end{cases} \tag{4}$$

where θ_{ij} is the misorientation between cell i and cell j, and θ^* is the misorientation limit for low angle boundaries which is set as 15, J is a linear boundary energy

density, it equals J_α if both of cell i and cell j belong to phase α, J_α if both cell i and cell j belong to phase γ and $J_{\alpha\gamma}$ if cell i and cell j belong to phase α and γ, respectively, where $J_{\alpha\gamma} = 0.80$ J/m^2, $J_\gamma = 0.79$ J/m^2, $J_{\alpha\gamma} = 0.56$ J/m^2 [31,32].

2.5. Nucleation model

During the process of continuous cooling, a number of ferrite nuclei are introduced into the system per MCS to simulate the nucleation of ferrite grains. The amount of the newly formed ferrite nuclei can be given by

$$n(T) = \int_{T_1}^{T_2} \frac{I(T')(1-f)}{Q} \mathrm{d}T', \tag{5}$$

where Q is the cooling rate, f is the volume fraction of the ferrite, I_F is the nucleation rate of ferrite grains, which can be determined as follows [23,33–35]:

$$I_F = K_1 D_{C\gamma} (kT)^{-1/2} \exp\left(-\frac{K_2}{kT(\Delta G_N^{\gamma\to\alpha+\gamma})^2}\right), \tag{6}$$

where R is the mol gas constant, T is the temperature in Kelvin, K_1 and K_2 are two composition independent constants, which can be determined as $K_1 = 2.07 \times 10^3$ J$^{1/2}$ cm^{-4} and $K_2 = 6.33 \times 10^{-15}$ J^3 mol^{-2} according to reference [35], $D_{C\gamma}$ is the diffusion coefficient of carbon atoms in the austenite, which can be expressed as follows according to the work of Kaufman et al. [36]:

$$D_{C\gamma} = 0.5 \exp(-30 x_C^\gamma) \exp\left(-\frac{Q_D}{RT}\right),$$

$$Q_D = 38,300 - 190,000 x_C^\gamma + 550,000 (x_C^\gamma)^2,$$

where $\Delta G_N^{\gamma\to\alpha+\gamma}$ is the nucleation driving force of ferrite grains, which can be determined as follows according to the super lattice model [34]:

$$\Delta G_{N(S)}^{\gamma\to\alpha+\gamma} = \Delta G_S^{\gamma\to\alpha} - RT \ln a_s^\gamma,$$

$$\Delta G_S^{\gamma\to\alpha} = 141 \sum x_i (\Delta T_M^i - \Delta T_{NM}^i) + \Delta G_{Fe(S)}^{\gamma\to\alpha},$$

where $\Delta G_{Fe(S)}^{\gamma\to\alpha}$ is the free energy difference of pure iron between the ferrite and the austenite, a_s^γ is the activity of the austenite which can be determined by the work of Xu et al. [37,38], ΔT_M^i and ΔT_{NM}^i are two Zener parameters for element i.

3. Simulation

The composition of a low carbon steel (C 0.14, Si 0.20, Mn 0.49, P 0.014, S 0.013, Cu 0.01, Al 0.02) is adopted as the nominal composition of the system in the simulation. The data presented in the following sections are obtained by averaging over five simulations under identical simulation conditions. To verify the simulation, some experimental results are included in this paper. In the experiments, the specimens were austenited at 1223 K for 10 min and then cooled at different cooling rates. The specimens were polished and etched using nital for taking the optical metallograph and the quantitative metallography analysis.

3.1. The initial polycrystalline microstructure of the system in the simulation

The system is a square domain with 100×100 MC cells in the simulation. The microstructure is obtained from the MC simulation result of normal grain growth. At the beginning of the simulation, each MC cell is assigned to belong to the austenite with a homogeneous nominal composition. This initial microstructure is displayed in Fig. 2. Periodic boundary condition is adopted.

3.2. Effect of the cooling rate on the volume fraction of the ferrite

In the simulation, the effect of the cooling rate on the volume fraction of the ferrite is investigated by cooling the system at different cooling rates. As can be seen from Fig. 3, the volume fraction of the ferrite decreases as the cooling rate increases. This phenomenon arises from the restraining effect of the increase of the cooling rate on the diffusion of the carbon atoms. The austenite–ferrite diffusive transformation is dominated by the boundary migration and the carbon diffusion. The carbon diffusion is time consuming. When the cooling rate is increased, the duration for the carbon atoms to diffuse is shortened. The insufficiency of the diffusion of the car-

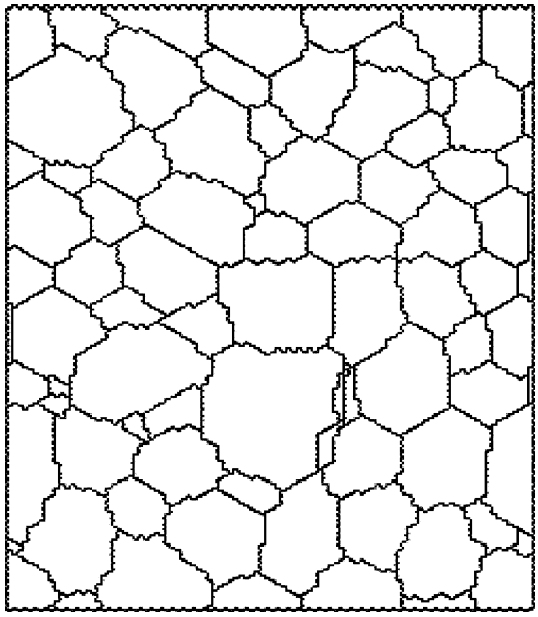

Fig. 2. Initial microstructure of the system.

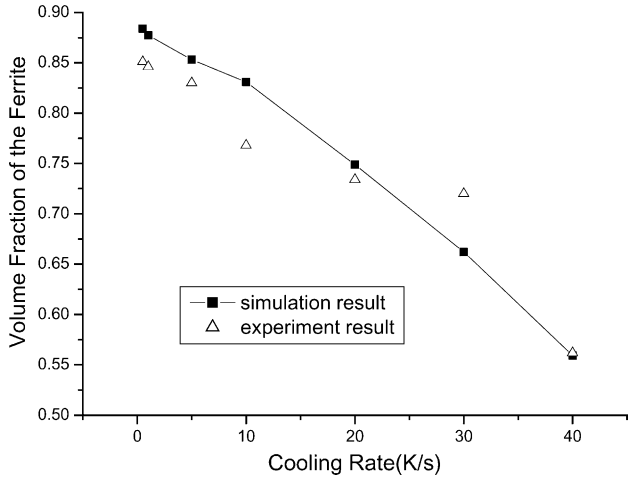

Fig. 3. Volume fraction of ferrite at different cooling rates.

bon atoms restrains the transformation from the austenite to the ferrite. Therefore, the volume fraction of the ferrite is decreased by the increase of the cooling rate. The experimental result of the volume fraction of the ferrite as a function of the cooling rate is also shown in Fig. 3 to verify the simulation result. Fig. 3 shows that the calculated volume fraction of ferrite agrees well with the corresponding experimental result.

3.3. Effect of the cooling rate on the ferrite grain size

The simulation result of the effect of the cooling rate on the mean ferrite grain size is shown in Fig. 4. As the cooling rate increases, the mean interception of the ferrite grains decrease gradually. This means that accelerating the cooling process refines the microstructure. The grain refinement effect of accelerating the cooling process comes from the effect of the cooling rate on the nucleation and the growth of ferrite grains. In the simulation, the nucleation of ferrite grains proceeds in the manner of probability. The nucleation probability of an austenite MC cell is proportional to the nucleation rate. A large cooling rate results in a large undercooling temperature in the austenite grains, which dramatically increase the nucleation rate. Thus, the nucleation probability is increased by the increase of the cooling rate. The increase of the cooling rate, at the same time, dramatically shortens the duration that the system experienced at a high temperature (upward of 773 K). Therefore, the grain growth of ferrite grains is restrained by the increase of the cooling rate. The promoting effect of the increase of the cooling rate on the nucleation of ferrite grains and the restraining effect of it on the growth of ferrite grains refine the microstructure. Fig. 4 shows that the simulation result of the effect of the cooling rate on the mean ferrite grain size agrees well with the corresponding experimental result.

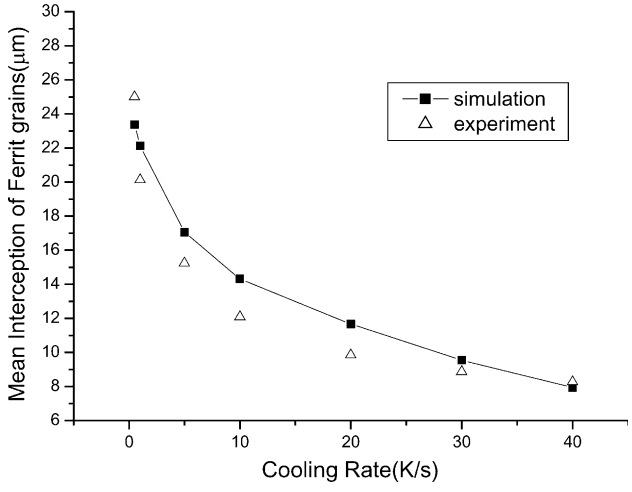

Fig. 4. Comparison between the calculated mean ferrite grain size of the system at different cooling rates and the experimental one.

3.4. The evolution of the carbon concentration field of the system cooled at 0.5 K/s

The carbon diffusion is one of the important objects that are investigated in the simulation. Fig. 5(a)–(d) shows the evolution of the carbon concentration field as the system is cooled at the cooling rate of 0.5 K/s. It is obvious that the carbon diffuses from the ferrite grains to the neighboring austenite grains as the nucleation and the growth of ferrite grains proceeds. The carbon diffusion from the ferrite grains to the neighboring austenite grains makes the carbon rich near phase boundaries of the austenite grains and makes the carbon poor near phase boundaries of the ferrite grains. Accompanied by the poorness of carbon in the ferrite grains, the richness of carbon in the austenite grains and the migration of phase boundaries, the volume fraction of the ferrite increases gradually. As the transformation proceeds, the carbon richness and the carbon poorness approach to the interiors of the austenite grains and the ferrite grains, respectively.

3.5. Transformation kinetics of the systems cooled at different cooling rates

The transformation kinetics of the systems during the process of continuous cooling at different cooling rates is shown in Fig. 6. The transformation kinetics curves can be divided into two groups. One group contains the systems cooled at low cooling rate (including 0.5 and 1 K/s), the other group contains the systems cooled at high cooling rate (including from 5 to 40 K/s). The volume fractions of the ferrite of the systems in the group with low cooling rates gradually saturate at the late stage of phase transformation process. When the system is cooled at a very low cooling rate, the system is very close to its equilibrium state. The carbon atoms

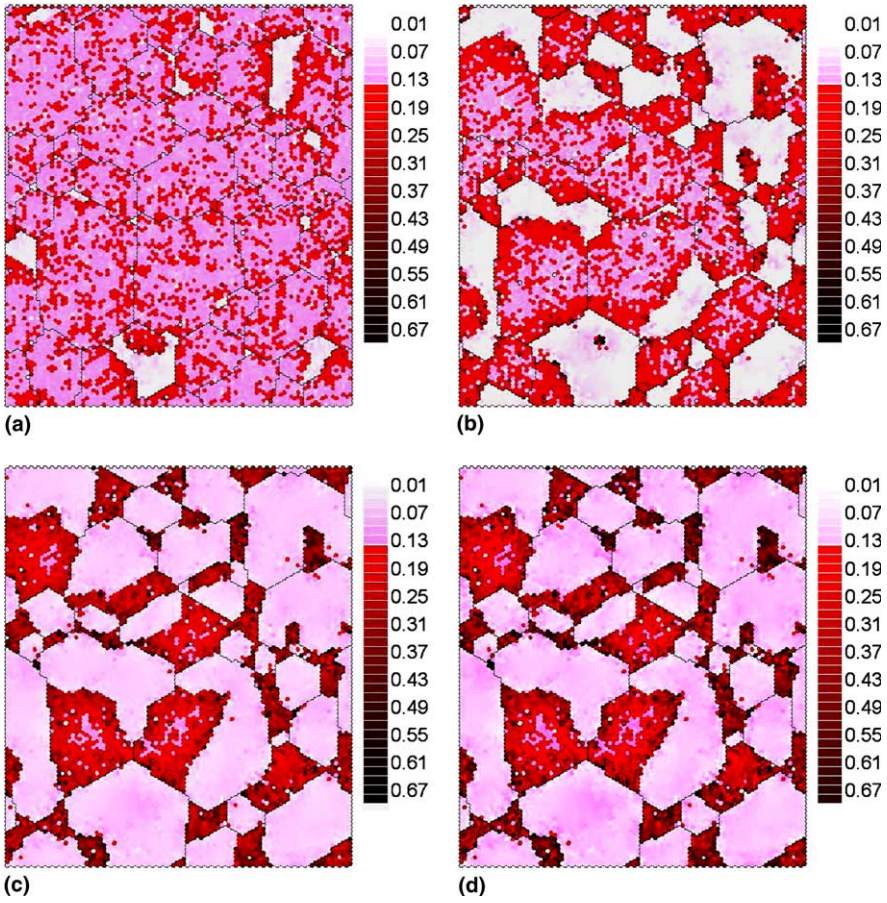

Fig. 5. Carbon concentration field of the system cooled at the cooling rate of 0.5 K/s at: (a) 1048; (b) 1038; (c) 1028; (d) 983 K.

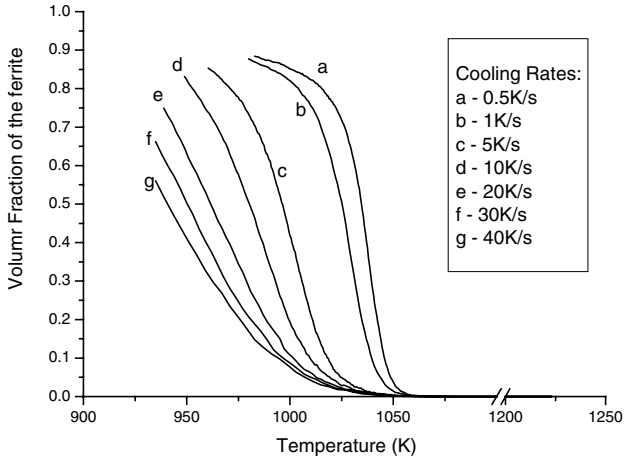

Fig. 6. Simulation result of the transformation kinetics of the system at different cooling rates.

diffuse sufficiently. At the late state of the phase transformation, the nucleation and the growth of ferrite grains are gradually slowed down by the dramatic richness of the carbon concentration in the austenite grains. When the system is cooled at a high cooling rate, however, the system is far away from its equilibrium state. The carbon diffusion is not sufficient. The nucleation and the growth of the ferrite grains still proceed fast at the late stage of the transformation. Thus, the transformation proceeds still fast till the end of it as shown in the curves in the group with low cooling rates.

3.6. Microstructure of the system cooled at the cooling rate of 0.5 K/s

The simulation result of the morphology of the microstructure is displayed in Fig. 7(a). The white regions represent the ferrite grains and the black regions represent the pearlite. The ferrite grains are all polygonal. This morphology agrees well with the metallograph of the sample cooled at the cooling rate of 0.5 K/s in the experiment, which is shown in Fig. 7(b).

3.7. The effect of the interfacial energy on the transformation

In the finite volume method based CA simulations [10–13], the effects of the interfacial energy on the transformation are neglected. The CA simulation results show that almost all the simulated ferrite grains are not of polygonal but irregular figure. There are numerous

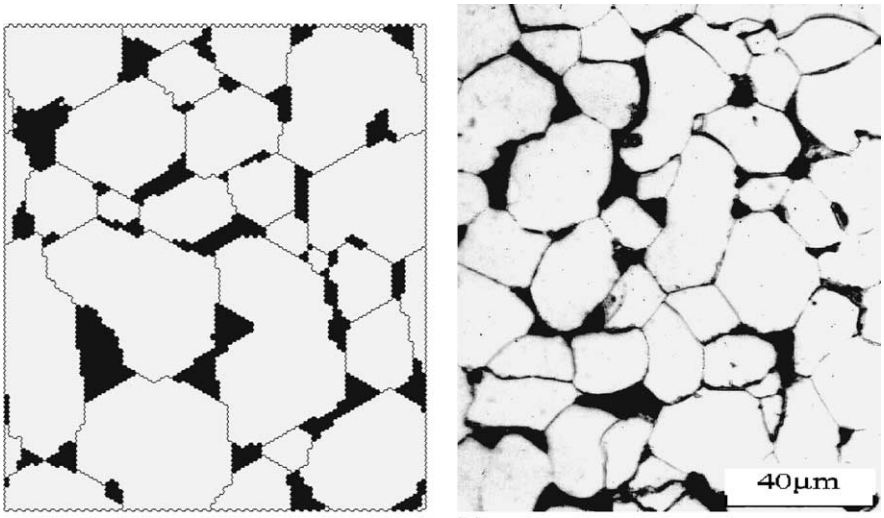

Fig. 7. (a) Calculated microstructure of the system at the cooling rate of 0.5 K/s. (b) Metallograph of the microstructure of sample cooled at the cooling rate of 0.5 K/s in the experiment.

sentusi along the ferrite grain boundaries. Most of the dihedrals between two ferrite grain boundaries at the triple junctions deviate 120 far way. This morphology of the ferrite grains simulated by the CA model is not in accordance with the experimental result shown in Fig. 7(b) and the general knowledge about the morphology of the microstructure. As is known to all, in reality, the two-dimensional ferrite grain boundaries should be plane and smooth and the dihedrals between two grain boundaries at the triple junctions should be 120. The questionable morphologies simulated by the CA models are directly brought about by the neglect of the effect of the interfacial energy on the microstructure. In fact, the interfacial energy significantly affects the morphology of the microstructure. As a whole, the interfacial energy takes effect on the morphology of the microstructure by dint of the minimization tendency of the interfacial energy. The minimization tendency of the interfacial energy mainly results in two phenomena. The first one is to make the ferrite grain boundaries plane and eliminate the sentusi to minimize the total boundary area. The second one is to make the dihedrals between two ferrite grain boundaries at the triple junctions to be to keep the triple junctions balance. Because the interfacial energy is not taken into account in the CA model, there is no minimization tendency of the interfacial energy in the CA simulations. Though Krielaart and coworkers [39] adopted the interfacial energy in the form of the interface mobility M in their CA simulation as follows:

$$v = M\Delta\mu_{\mathrm{Fe}}, \tag{7}$$

$$M = M_0 \exp\left(-\frac{E}{RT}\right),$$

where v is the interface velocity, $\Delta\mu_{\mathrm{Fe}}$ is the chemical potential difference of iron, E is the activation energy, the interfacial energy is not able to affect the morphology of the ferrite grains because the interface mobility is a uniform constant for all the CA cells at a given temperature and there is no minimization tendency of the interfacial energy in the CA model yet. The neglect of the interfacial energy effect makes the CA simulation results of the morphology of the microstructure questionable. In the present paper, the effect of the interfacial energy on the transformation is taken into account via the interfacial energy term in the Hamiltonian of the system in the MC simulation. The movement of the boundaries proceeds in a Metropolis sampling manner. The interfacial energy term in the Hamiltonian brings bout the minimization tendency of the interfacial energy via the Metropolis sampling. Thus, the ferrite grains are gradually made to be polygonal and the sentusi are removed by the minimization tendency of the boundaries area. As can be seen in Fig. 7(a), the ferrite grains produced by the MC simulation are all polygonal and the ferrite grain boundaries are all smooth. Moreover, most of the dihedrals of the ferrite grain boundaries at the triple junctions are very close to 120. The simulated morphology of the microstructure agrees well with the experimental result shown in Fig. 7(b). The consideration of the interfacial energy effect makes the MC simulation results of the morphology of the microstructure seem more reasonable than those simulated by the CA model. As a whole, by considering the interfacial energy effect, the capability of reasonably simulating the morphology of the microstructure is the most significant advantage of the MC simulation over the CA simulation.

4. Summary

By taking the interfacial energy and the chemical free energy into account, a Q-state Potts model is used to simulate the austenite–ferrite diffusive transformation in a low carbon steel during continuous cooling on a mesoscale with MC method. The consideration of the interfacial energy effect makes the simulated ferrite grains polygonal. The ferrite grain boundaries are all plane and smooth. Most of the dihedrals between two ferrite grain boundaries at the triple junctions are very close to 120 in the MC simulation. The morphology of the microstructure agrees well with the experimental results. The effect of the cooling rate on the microstructure is simulated. Because the carbon diffusion is time consuming, increasing the cooling rate decreases the volume fraction of the ferrite. By promoting the nucleation of the ferrite grains and restraining the growth of them, increasing the cooling rate dramatically decreases the mean ferrite grain size. The cooling rate takes obvious effect on the transformation kinetics. The volume fraction of the ferrite gradually saturates when the system is cooled at a low cooling rate. This saturation, however, does not occur when the system is cooled at a high cooling rate. The evolution of the carbon concentration field of the system during continuous cooling is simulated. Accompanied by the nucleation and the growth of the ferrite grains, the carbon diffuses from the ferrite grains to the austenite grains. There exist obvious carbon richness near the phase boundaries of the austenite grains and corresponding carbon poorness near the phase boundaries of the ferrite grains. As the decomposition of the austenite grains proceeds, this carbon richness and carbon poorness gradually approach to the interiors of the austenite grains and those of the ferrite grains, respectively. This carbon diffusion simulation is independent on the numerical solution of the diffusion equation.

Acknowledgements

The authors express their thanks to Professor Jun Ni in Tsinghua University (Department of Physics) for helpful discussions. This research work is financially supported by National Key Program of Basic Research Development of China under Grant No. GT1998061512.

References

[1] Leblond JB, Devaux J. Acta Metall 1984;32:137.
[2] Denis S, Farias D, Simon A. ISIJ Int 1992;32:316.
[3] Pham TT, Hawbolt EB, Brimacombe JK. Met Trans 1995;26A:1987.
[4] Karlsson B, Larsson LE. Mater Sci Eng 1975;20:161.
[5] Akbay T, Reed RC, Atkinson C. Acta Met 1994;47:1469.
[6] Inoue K, Ohmura E, Haruta K, Ikuta S. Trans JWRI 1987;16:49.
[7] Inoue K, Ohmura E, Ikuta S. Trans JWRI 1987;16:97.
[8] Jacot A, Rappaz M. Acta Metall 1997;45:575.
[9] Jacot A, Rappaz M. Acta Metall 1999;47:1645.
[10] Kumar M, Sasikumar R, Kesavan Nair P. Acta Metall 1998;46:6291.
[11] Zhang L, Zhang CB, Zhang YM, Liu XH, Wang GD. J Mater Res 2002;17:2251.
[12] Zhang L, Zhang CB, Wang YM, Wang SQ, Ye HQ. Acta Metall 2003;51:5519.
[13] Zhang L, Wang YM, Zhang CB, Wang SQ, Ye HQ. Modelling Simul Mater Sci Eng 2003;11:791.
[14] Srolovitz DJ, Anderson MP, Grest GS, Sahni PS. Acta Metall 1984;32:783;
Acta Metall 1984;32:793;
Acta Metall 1984;32:1429;
Acta Metall 1985;33:509;
Acta Metall 1985;33:2233.
[15] Radhakrishnan B, Sarma GB, Zacharia T. Acta Metall 1998;46:4415.
[16] Rollett AD, Luton MJ, Srolovitz DJ. Acta Metall 1992;40:43.
[17] Xu Zuyao. Phase transformation theory [in Chinese]. Beijing: Science Press; 1998. p. 64.
[18] Xu Zuyao. Acta Metall Sinica 1985;21:107.
[19] Kaufman L, Radeliffe SV, Cohen M. In: Zackey VF, Aaronson HI, editors. Decomposition of austenite by diffusional process. New York: Interscience; 1962. p. 313.
[20] Shiflet GJ, Bradley JR, Aaronson HI. Metall Trans 1978;9A: 999.
[21] Aaronson HI, Domain HA, Pound GM. Trans Metall Soc AIME 1966;236:753.
[22] Lobo JA, Greiger GH. Metall Trans 1976;7A:1347.
[23] Liu Zhenyu, Thesis for Doctor's Degree. Northeast University, Shenyang, 1995, 46pp.
[24] Weiss RJ, Tauer KJ. Phys Rev 1956;122:1490.
[25] Metals handbook, 9th ed., vol. 741. Metals Park (OH): ASM International; 1988.
[26] Liang Yingjiao, Che Yinchang. Mineral thermodynamics handbook [in Chinese]. ShenYang: NorthEasten University Press; 1993. p. 146.
[27] Kaufman L, Clougherty EV, Weiss RJ. Acta Metall 1963;11: 323.
[28] Liang Yingjiao, Che Yinchang. Thermal data hand book of inorganics [in Chinese]. Shen Yang: Northeast University Press; 1993. p. 230.
[29] Srest GS, Srolovitz DJ, Anderson MP. Acta Metall 1985;33:509.
[30] Radhakrishnan B, Sarma GB, Zacharia T. Acta Metall 1998;46:4415.
[31] Song Yujiu. The relationship between the grain boundaries and the strength of metals [in Chinese]. Xian Jiao Tong University Press; 1987. p. 46.
[32] Chen Jiqin, Chen Minxiong, Zhao Jingshi. Crystal defects [in Chinese]. Zhe Jiang University Press; 1992. p. 174.
[33] Lange WF, Enomoto M, Aaronson HI. Metall Trans A 1988;19:427.
[34] Translated by Wang Guodong, Liu Zhenyu, Xiong Shangwu, Controlled rolling and controlled cooling of HSLA steel. Beijing: Metallurgical Industry Press; 1993.
[35] Umemoto M, Zing Hai Guo, Tamura I. Mater Sci Technol 1987;3:249.
[36] Kaufman L, Radcliffe SV, Cohen M. In: Zackay VF, Aaronson HI, editors. Decomposition of austenite by diffusional process. Easton, Pennsylvania: TMS-AIME; 1962. p. 313.
[37] Zuyao Xu, Shikai Liu. Bainite transformation and bainite. Beijing: Science Press; 1991.
[38] Yiwen Mou, Zuyao Xu. Acta Metall 1986;34:325.
[39] Krielaart Gerben P, Jilt Sietsma, Sybrand van der Zwaag. Mater Sci Eng A 1997;237:216.